Proc. Natl. Acad. Sci. USA
Vol. 89, pp. 99–103, January 1992
Medical Sciences

The cardiac conduction system in the rat expresses the α2 and α3 isoforms of the Na^+,K^+-ATPase

(*in situ* hybridization/heart conduction system/atrioventricular node/Purkinje strand)

RAPHAEL ZAHLER*†, MICHAEL BRINES*, MICHAEL KASHGARIAN‡, E. J. BENZ, JR.*, AND MAUREEN GILMORE-HEBERT§

Departments of *Internal Medicine, ‡Pathology, and §Therapeutic Radiology, Yale University School of Medicine, 333 Cedar Street, New Haven, CT 06510

Communicated by Vincent T. Marchesi, September 5, 1991

ABSTRACT **The sodium pump is crucial for the function of the heart and of the cardiac conduction system, which initiates the heartbeat. The α (catalytic) subunit of this pump has three isoforms; the α1 isoform is ubiquitous, but the α2 and α3 isoforms are localized to excitable tissue. Because rodent α2 and α3 isoforms are relatively sensitive to ouabain, which also slows cardiac conduction, we studied heart-cell-specific expression of pump isoform genes. Multiple conduction-system structures, including sinoatrial node, bundle branches, and Purkinje strands, had prominent, specific hybridization signal for α2 and α3 isoforms compared with adjacent working myocytes. This gene-expression approach may be useful for labeling conduction tissue and also for localizing specific membrane channels and receptors in this system.**

The sodium pump (Na^+,K^+-ATPase), a ubiquitous enzyme that extrudes sodium from the cell in exchange for potassium, has many important physiologic functions in the heart, such as regulation of cell volume, generation of ion gradients for solute transport, and maintenance of voltage gradients in excitable tissue. Digitalis glycosides, an important class of cardiac drugs, are highly specific inhibitors of this enzyme. Recently, Na^+,K^+-ATPase activity has been found to arise from a complex pattern of gene expression involving, at least, six loci. The functional enzyme is made up of distinct α and β protein chains and possibly a third γ subunit; the α subunit has three isoforms, and the β subunit has, at least, two isoforms. All three α isoforms are expressed in mammalian heart in developmentally complex ways (1–4). Thus, recently discovered changes (both regional, developmental, and pathophysiologic) in Na^+,K^+-ATPase isoform distribution (5, 6) are likely to be important in cardiac physiology.

A complex cell-type-specific distribution of isoforms is already known to occur in several tissues, including brain and transport epithelia (7–9) at both the mRNA and protein levels (10). In the heart, as in most tissues, α1 is the predominant α isoform; yet the pattern of developmental change and response to stimuli are complex for the other isoforms. Although not all previous workers found α3 isoform in rat heart, recent data indicate that high-affinity isoform protein is present in this tissue despite the overall low glycoside sensitivity, suggesting that the isoenzymes may differ in their contribution to cardiac physiology (11). We and others have shown regional variations in isoform gene expression in both normal and pressure-overloaded heart (12–15), but the significance of these changes is unknown.

The cardiac conduction system is responsible for the initiation and propagation of the heartbeat. Because in adult animals α3 isoform is found almost exclusively in the central nervous system, we suspected that this isoform is preferentially expressed in specialized cardiac conduction tissue. This conjecture is reasonable because (*i*) the cardiac effects of glycosides are especially prominent in the conduction system (although this action is also mediated indirectly via the nervous system), (*ii*) Purkinje fibers contain pumps that are more ouabain-sensitive than those of ventricular muscle, both by electrophysiologic and transport criteria (16–18), (*iii*) electrophysiologic parameters have been found to differ between Purkinje myocytes and working ventricular fibers (19–22). We thus used the technique of *in situ* hybridization to address this issue.

MATERIALS AND METHODS

We used hearts from adult male rats to prepare the histologic sections. Sprague–Dawley rats (Charles River Breeding Laboratories) were anesthetized with enflurane, and hearts were removed through a midline thoracotomy. Hearts were immersed in 4% (wt/vol) paraformaldehyde/phosphate-buffered saline for 2 hr and 15% sucrose/phosphate-buffered saline for 3 hr (both at 4°C) and then bisected through the long axis. These tissues were then embedded in OCT, frozen in isopentane, and stored at −70°C until use. Frozen sections (10 μm) were cut at −20°C, thaw-mounted, and then frozen at −70°C.

Isoform-specific antisense oligonucleotides (30-mers) for the α isoforms were synthesized as described (8, 9) in such a way that each oligonucleotide has 100% homology with the corresponding Na^+,K^+-ATPase isoform, but cross-homology between α isoform-specific oligonucleotides is <23%. The specificity of these probes has been previously validated by Northern (RNA) analysis (8). Because we had difficulty achieving low background with the α1 oligonucleotide probe, labeled RNA probe was prepared from a rat α1 isoform fragment (23). This fragment, cloned into the pGEM4 vector, was linearized and shortened by digestion with *Nco* I and *Bam*HI. Labeled RNA probe was synthesized as described (24). Oligonucleotides were 3′-end-labeled with poly(adenosine [^{35}S-thio]triphosphate) using terminal transferase (New England Nuclear). Probes were diluted so that each section received 3×10^5 dpm.

In all experiments, pairs of slides with serial sections were processed at the same time in the same solutions, with one slide of each pair incubated with antisense probe and the other slide incubated with control probe. Paired slides were also exposed and developed together. Following the procedure of Wilcox *et al.* (25), slides were thawed, fixed in 4% paraformaldehyde/phosphate-buffered saline at 4°C, and washed in 0.5× standard saline citrate buffer before and after deproteination with 0.2 M HCl. For prehybridization, each section was covered with 50 μl of hybridization buffer [RNA probes: 50% (vol/vol) formamide/0.3 M NaCl/20 mM Tris/5

The publication costs of this article were defrayed in part by page charge payment. This article must therefore be hereby marked "*advertisement*" in accordance with 18 U.S.C. §1734 solely to indicate this fact.

†To whom reprint requests should be addressed.

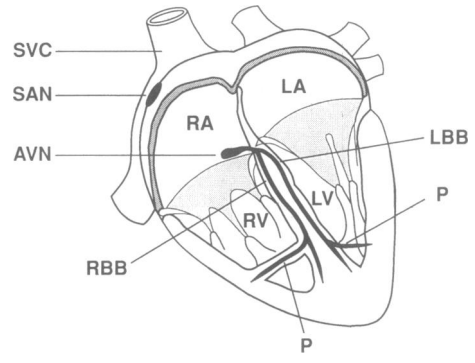

FIG. 1. Sketch of cardiac conduction system. SVC, superior vena cava; SAN, sinoatrial node; AVN, atrioventricular node; RBB/LBB, right/left bundle branches; P, Purkinje strand; LV, left ventricle; RV, right ventricle; LA, left atrium; RA, right atrium.

mM EDTA/1× Denhardt's solution/10% dextran sulfate/10 mM dithiothreitol; oligonucleotide probes: 30% (vol/vol) formamide/2× standard saline citrate/1× Denhardt's solution/10% dextran sulfate/salmon sperm DNA at 100 μg/ml, yeast tRNA at 100 μg/ml/10 mM dithiothreitol], placed in a humidified box, and incubated for 1–3 hr. Then, 10 μl of labeled probe was added directly to the buffer overlying each section, and the slides were incubated overnight at 55°C (RNA probes) or 37°C (oligonucleotide probes)—5°C lower than the calculated melting temperature T_m. After hybridization, slides were treated with RNase A (RNA probes only) for background reduction and were washed in 0.2× standard saline citrate/10 mM mercaptoethanol/1 mM EDTA for 2 hr at 65°C (RNA probes) or 1.5 hr at 60°C (oligonucleotide probes). The slides were dehydrated, dried, coated with Ilford K-4 emulsion (Polysciences), and exposed for 7–21 days. Slides were then developed in Kodak D-19 solution, counterstained with hematoxylin/eosin, and photographed both by conventional light microscopy and with a confocal epipolarization microscope system (Bio-Rad).

RESULTS

The main structures of the cardiac conduction system are shown in Fig. 1: the impulse is initiated in the sinoatrial node, travels through the atrioventricular node, and spreads through the right and left bundles to the Purkinje fibers, which form strands branching out from the endocardium adjacent to the papillary muscles of both ventricles. At the level of the Purkinje strands (Figs. 2 and 3), we observed hybridization signal for the α2 and α3 probes in the specialized conducting cells, which are round and pale-staining but not in the more elongated, striated working muscle cells. Fig. 2*B* also shows that cells in the Purkinje strand and immediate subendocardial area have much more intense α2 signal than those deeper in the septal myocardium, again suggestive of conduction-system localization.

The sinoatrial node, a discrete structure at the junction of superior vena cava and right atrium (Fig. 4 *A* and *B*, straight arrows) also has intense signal for the α2 isoform when compared with neighboring vascular and atrial tissue (curved arrows). In the region of the right and left bundle branches (Fig. 5*A*), the conduction tissue is recognizable as subendocardial bands of lighter-staining cells (arrows). High-power views of these bands probed for α3 isoform (Fig. 5 *B* and *C*) show deposition of silver grains in a linear pattern (arrows), consistent with α3 mRNA in the right bundle (a linear pattern of increased α3 signal was also seen in the left bundle, and both bundles were also positive for α2 isoform; data not

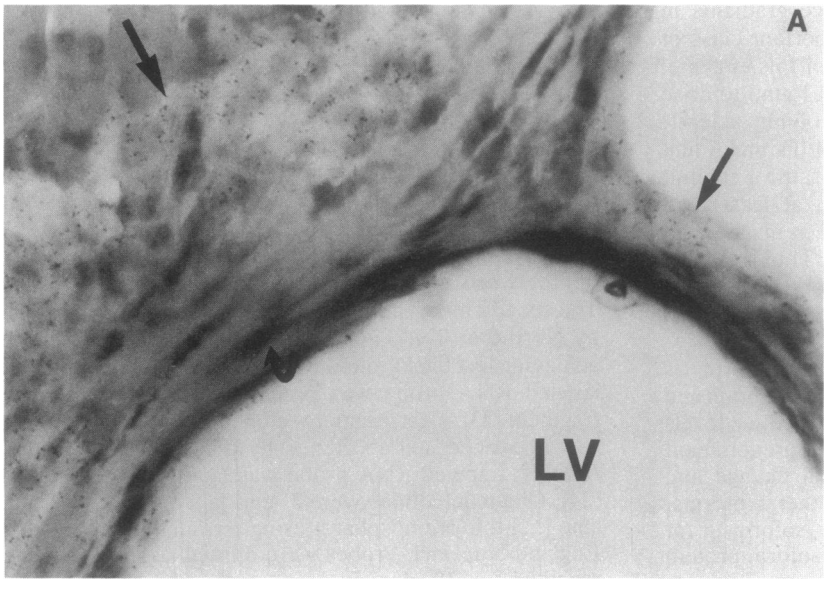

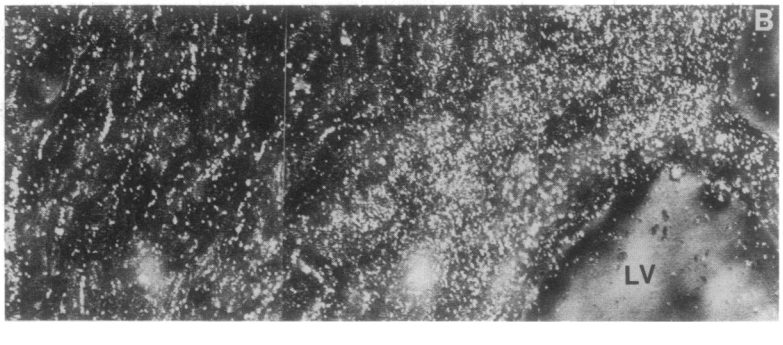

FIG. 2. Purkinje strand, branching from septum into left ventricular (LV) cavity, probed for α2 isoform. (*A*) Transmission photograph, showing silver grains as black dots. Straight arrows, specialized conducting cells; curved arrow, striated muscle cell. (×2400.) (*B*) Lower-power dark-field confocal image (montage of three frames), showing silver grains as white dots. (×1550.)

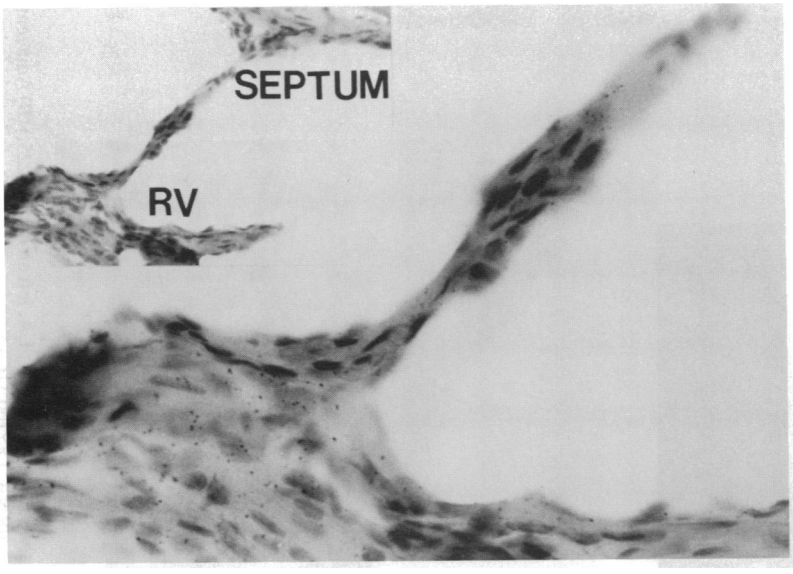

FIG. 3. Purkinje strand branching from septum to right ventricle (RV), probed for $\alpha 3$ isoform. (×2300.) (*Inset*) Bridging from septum to RV free wall.

shown). As a control, Fig. 5*D* is an adjacent section incubated in parallel with the same amount of labeled $\alpha 2$ oligonucleotide plus an excess of unlabeled $\alpha 2$ oligonucleotide; this competition abolishes the hybridization signal. In addition, round pale-staining cells in the interatrial septum, possibly representing atrioventricular-nodal tissue or His bundle, have markedly increased $\alpha 2$ and $\alpha 3$ activity (data not shown).

To confirm the findings shown in these figures, grains were counted manually in four regions of different slides. In each case, signal per unit area was 3- to 5-fold higher in areas of conduction tissue than in adjacent working myocardial cells ($P < 0.002$ for each comparison by Student's t test).

Controls for nonspecific binding of probe to tissue sections included sense RNA probe of the same activity as the antisense RNA probe, which showed very low levels of labeling (Fig. 6), and competition slides (for oligonucleotide probes), which received labeled oligonucleotide, together with an excess of the identical, unlabeled, oligonucleotide (Fig. 5*D*). Moreover, only the $\alpha 1$ probe hybridized to the thick ascending limb of rat kidney (which is known to have high levels of $\alpha 1$ message) under the conditions of these experiments (data not shown). In addition, as noted above, conduction-tissue cells consistently showed more signal with $\alpha 2$ and $\alpha 3$ probe than adjacent working muscle, indicating that our results were not artifacts of uneven distribution of probe or emulsion thickness.

In contrast to $\alpha 2$ and $\alpha 3$, the $\alpha 1$ isoform shows substantial *in situ* hybridization signal in working myocardium (Fig. 6), but Purkinje strands do not have increased levels of $\alpha 1$ message compared with muscle fibers (data not shown). Although this $\alpha 1$ data was obtained using RNA probe and not oligonucleotide probe, data from Northern analysis (2, 5, 7) indicate that any $\alpha 2$ and $\alpha 3$ cross-reactivity would make up only a small fraction of the $\alpha 1$ RNA probe signal.

DISCUSSION

We have demonstrated specific localization of $\alpha 2$ and $\alpha 3$ mRNA to the rat cardiac conduction system at multiple levels. Hybridization signal for these isoforms corresponded to locations where one would expect to see conduction tissue. More specifically, in these locations, those cells that had microscopic morphology suggestive of conduction tissue showed markedly increased hybridization signal compared with adjacent cells (Fig. 2). Further, when morphology of individual cells was ambiguous (Fig. 4), increased signal, confirmed by grain counts, was observed in those areas (identified by gross-anatomical landmarks) in which conduction-system tissue should occur. In contrast, the $\alpha 1$ isoform was expressed at high levels in working myocardium, without notable increases in Purkinje strands.

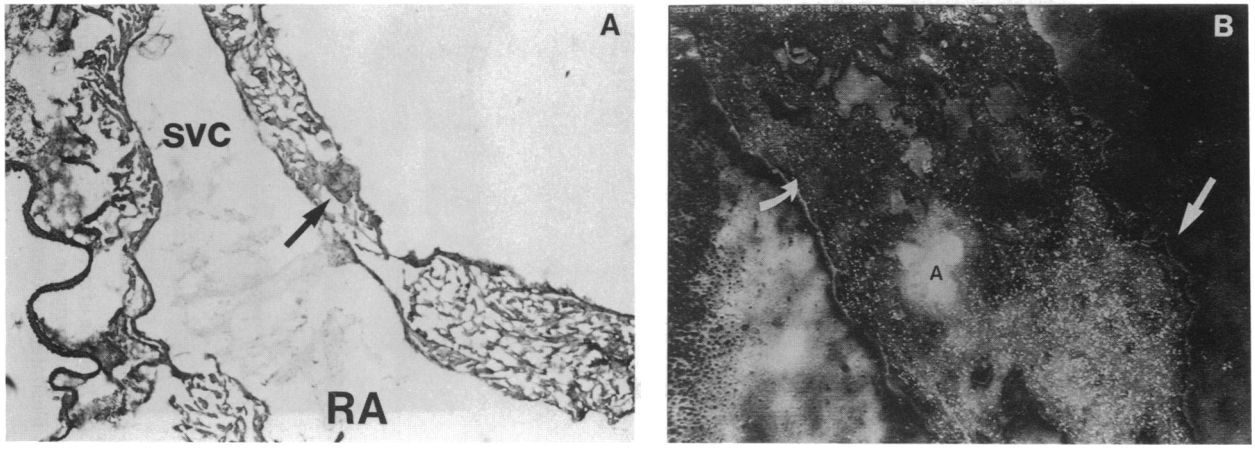

FIG. 4. (*A*) Low-power view of sinoatrial node (straight arrow) as identified by gross-anatomical landmarks (SVC, superior vena cava; RA, right atrium). (×180.) (*B*) Dark-field image of sinoatrial node (straight arrow) probed for $\alpha 2$ isoform; A, confocal laser artifact. (×1100.) Curved arrow, vascular and atrial tissue.

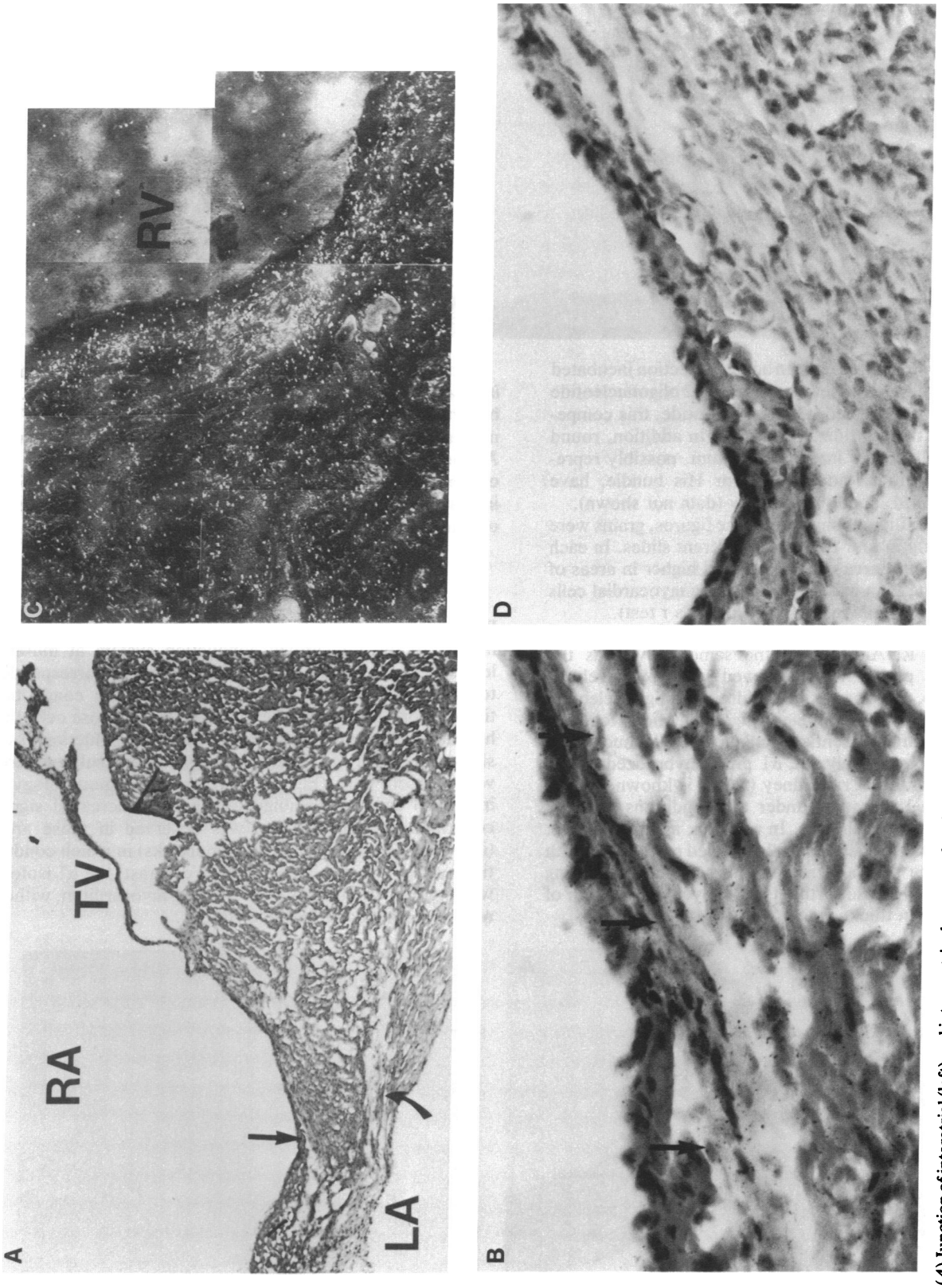

FIG. 5. (*A*) Junction of interatrial (left) and interventricular septa, showing bundle branches. Arrows, conduction tissue. TV, triscuspid valve; RA, right atrium; LA, left atrium. (×225.) (*B*) Adjacent section to *A*, right ventricular subendocardium, probed for $\alpha 3$ isoform. Arrows, linear pattern of silver grain deposition, consistent with $\alpha 3$ mRNA. (×2100.) (*C*) Same section as *B*, dark-field image (montage), illustrating concentration of silver grains in a subendocardial band. (×825.) (*D*) Adjacent section to *A*, probed with $\alpha 2$ isoform plus excess unlabeled $\alpha 2$ oligonucleotide. (×1625.)

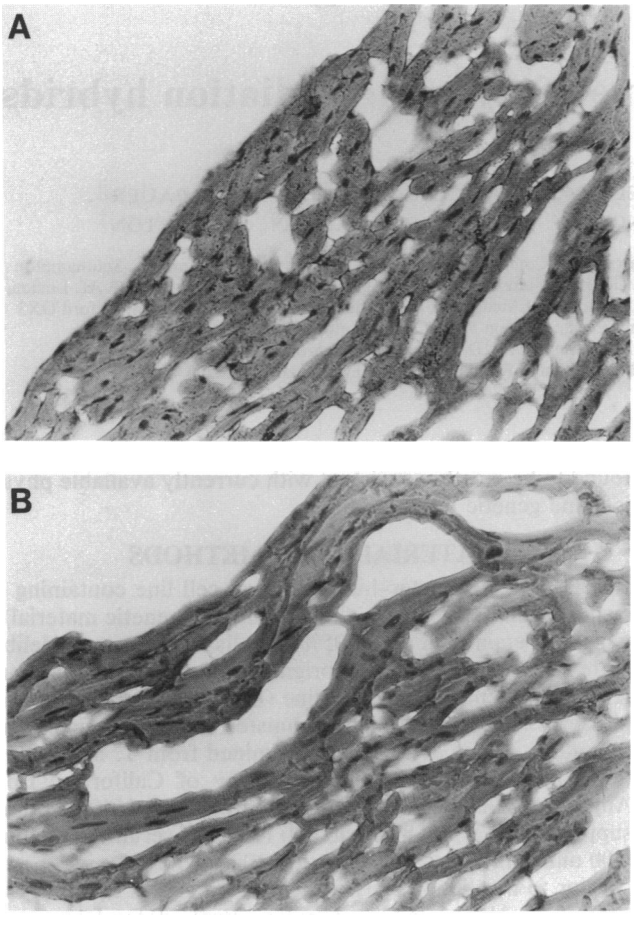

FIG. 6. Ventricular muscle incubated with α1 antisense (*A*) and sense (*B*) RNA probes at same number of dpm. (×1150.)

Because levels of sodium pump mRNA do not necessarily correlate with steady-state levels of mature protein, it will now be necessary to determine localized levels of subunit proteins and membrane-bound mature pump molecules in an isoform-specific fashion, preferably in parallel with electrophysiologic studies. In addition, our results may not be directly extensible to other species, because rodents differ from larger animals in the high ouabain resistance of their α1 form, and both adult human and dog—but not rat—hearts normally express major amounts of α3 isoform.

It is conceivable that increased signal was seen in conduction tissue compared with working muscle cells because the former have a lower content of contractile proteins and, thus, might allow better penetration of probe. This situation is an unlikely explanation for our findings, however, because (*i*) the RNA probe for α1 isoform penetrated working myocardium without difficulty in a specific fashion (Fig. 6) and yet is 10 times larger than the oligonucleotide probes used for α2 and α3 isoforms; (*ii*) differences between isoforms in deposition patterns were seen, even though the probes for different isoforms were the same size and processed identically: thus, α2, but not α3, isoform localized prominently to vessel wall (unpublished data); (*iii*) previously reported RNA blotting studies (1, 5) show that rat myocardium expresses much less α2 than α1 isoform and expresses α3 isoform at low-to-undetectable levels, so the low level of silver grains seen over muscle cells probably represents appropriate washing conditions. Thus, our findings cannot be explained by differences in probe penetration. Although cardiac conduction tissue is more richly innervated than working myocardium, it is unlikely that the *in situ* hybridization signal arises from nerve tissue because Na^+,K^+-ATPase mRNA is found in neuron cell bodies, as opposed to the nerve termini that predominate in conduction system.

Our data also indicate that $\alpha 2/\alpha 3$ *in situ* hybridization could be used as a "stain" or marker for the conduction system. This result may be important because cells of the cardiac conduction system are sometimes difficult to distinguish morphologically from working muscle fibers, leading to controversy about the exact location of specific pathways (26). Thus, our methods might allow more precise anatomic studies of the normal conduction system, as well as of bypass tracts, in postmortem animal and human tissue or allow the development of scintigraphic techniques to allow the *in vivo* visualization of the conduction system. Furthermore, the same oligonucleotide *in situ* hybridization techniques we used could be extended in a straightforward manner to define the conduction-system localization of mRNA for other important molecules, such as membrane channels or catecholamine receptors, for which the DNA sequence is known.

We thank Jo-San Chung, Paul Graham, and Drs. Fabian Chen, Josiah N. Wilcox, M. Utset, Ira S. Cohen, and Richard Eisen for advice and assistance. This work was supported, in part, by National Heart, Lung, and Blood Institute Clinical Investigator Award HL-01686.

1. Matsuda, T., Iwada, H. & Cooper, J. R. (1984) *J. Biol. Chem.* **259**, 3858–3863.
2. Sweadner, K. J. (1989) *Biochim. Biophys. Acta* **988**, 185–220.
3. Orlowski, J. & Lingrel, J. B. (1988) *J. Biol. Chem.* **263**, 17817–17821.
4. Orlowski, J. & Lingrel, J. B. (1988) *J. Biol. Chem.* **263**, 10436–10442.
5. Herrera, V. L., Chobanian, A. V. & Ruiz-Opazo, N. (1988) *Science* **241**, 221–223.
6. Maixent, J. M., Charlemagne, D., de la Chapelle, B. & LeLievre, L. G. (1987) *J. Biol. Chem.* **262**, 6842–6848.
7. Schneider, J. W., Mercer, R. W., Gilmore-Hebert, M., Utset, M. F., Lai, C., Greene, A. & Benz, E. J., Jr. (1988) *Proc. Natl. Acad. Sci. USA* **85**, 284–288.
8. Filuk, P. E., Miller, M. A., Dorsa, D. M. & Stahl, W. L. (1989) *Neurosci. Res. Commun.* **5**, 155–162.
9. Brines, M. L., Gulanski, B. I., Gilmore-Hebert, M., Greene, A. L., Benz, E. J., Jr., & Robbins, R. J. (1991) *Mol. Brain Res.*, in press.
10. Urayama, O., Shutt, H. & Sweadner, K. J. (1989) *J. Biol. Chem.* **264**, 8271–8280.
11. Lucchesi, P. A. & Sweadner, K. J. (1991) *J. Biol. Chem.* **266**, 9327–9331.
12. Ng, Y.-C. & Akera, T. (1987) *Am. J. Physiol.* **252**, H1016–H1022.
13. Charlemagne, D., Maixent, J. M., Preteseille, M. & Lelievre, G. (1986) *J. Biol. Chem.* **261**, 185–189.
14. Zahler, R., Gilmore-Hebert, M. & Benz, E. J., Jr. (1989) *Circulation* **80**, II–456.
15. Cutler, C. P. & Cramb, G. (1990) in *Proceedings 6th International Conference on the Sodium Pump* (Soc. Gen. Physiol., Woods Hole, MA), p. 64a.
16. Gao, J., Mathias, R. T., Cohen, I. S. & Baldo, G. J. (1991) *Biophys. J.*, in press.
17. Iacono, M. & Vassalle, M. (1990) *J. Pharm. Exp. Ther.* **253**, 1–12.
18. Somberg, J. C., Barry, W. H. & Smith, T. W. (1981) *J. Clin. Invest.* **67**, 116–123.
19. Baumgarten, C. M. & Fozzard, H. A. (1986) in *The Heart and Cardiovascular System*, ed. Fozzard, H. A. (Raven, New York), pp. 601–620.
20. De Mello, W. C. & Hoffman, B. F. (1960) *Am. J. Physiol.* **199**, 1125–1129.
21. Cohen, I. S., Datyner, N. B., Gintant, G. A., Mulrine, N. K. & Pennefether, P. (1987) *J. Physiol.* **383**, 251–267.
22. Nowak, G. & Haustein, K. (1976) *Pharmacology* **14**, 256–261.
23. Schneider, J. W., Mercer, R. W., Caplan, M., Emanuel, J. R., Sweadner, K. J., Benz, E. J., Jr., & Levenson, R. (1985) *Proc. Natl. Acad. Sci. USA* **82**, 6357–6361.
24. Gilmore-Hebert, M., Mercer, R. W., Schneider, J. W. & Benz, E. J., Jr. (1988) in *The Na,K Pump; Part B: Cellular Aspects*, eds. Skou, J. S., Norby, J. G., Maunsbach, A. B. & Esmann, M. (Liss, New York), pp. 71–76.
25. Wilcox, J. N., Smith, K. M., Williams, L. T., Schwartz, S. M. & Gordon, D. (1988) *J. Clin. Invest.* **82**, 1134–1140.
26. Sherf, L. & James, T. N. (1979) *Am. J. Cardiol.* **44**, 345–360.